Radiative Forcing of Quadrupling CO_2

MINGHONG ZHANG AND YI HUANG

Department of Atmospheric and Oceanic Sciences, McGill University, Montreal, Quebec, Canada

(Manuscript received 30 August 2013, in final form 4 December 2013)

ABSTRACT

An analysis method proposed by Huang is improved and used to dissect the radiative forcing in the instantaneous quadrupling CO_2 experiment from phase 5 of the Coupled Model Intercomparison Project (CMIP5). Multiple validation tests show that the errors in the forcing estimates are generally within 10%. The results show that quadrupling CO_2, on average, induces a global-mean all-sky instantaneous top-of-the-atmosphere forcing of $5.4\,W\,m^{-2}$, which is amended by a stratospheric adjustment of $1.9\,W\,m^{-2}$ and a tropospheric adjustment of $-0.1\,W\,m^{-2}$. The resulting fully adjusted radiative forcing has an ensemble mean of $7.2\,W\,m^{-2}$ and a substantial intermodel spread (maximum–minimum) of $2.4\,W\,m^{-2}$, which results from all the forcing components, especially the instantaneous forcing and tropospheric adjustment. The fidelity of the linear decomposition of the overall radiation variation is improved when forcing is explicitly estimated for each model. A significant contribution by forcing uncertainty to the intermodel spread of the surface temperature projection is verified. The results reaffirm the importance of evaluating the radiative forcing components in climate feedback analyses.

1. Introduction

In the analysis of climate sensitivity, it is a convention to consider radiative forcing to comprise both instantaneous forcing that is due to perturbation in radiative gases (e.g., CO_2) and contributions by rapid adjustments of other atmospheric components that are not related to surface temperature change (Ramaswamy et al. 2001). For instance, stratospheric temperature adjustment resulting from the radiative cooling effect of CO_2 is usually considered part of the CO_2 forcing (Hansen et al. 1997). Some recent studies also consider the rapid tropospheric adjustment of temperature, water vapor, cloud, and so on, as part of the forcing adjustment (Andrews and Forster 2008; Gregory and Webb 2008). It has been recognized that the strength of radiative forcing, as measured by modification of the top of the atmosphere (TOA) or tropopause radiation flux, may vary among different climate models even when the concentrations of these gases are identically prescribed (Collins et al. 2006; Dufresne and Bony 2008; Andrews et al. 2012; Webb et al. 2013; Forster et al. 2013; Huang 2013a). This forcing variation contributes to the difference in these models' projections of surface warming. When diagnosing climate projection experiments, this effect needs to be treated properly. Otherwise, the model feedback may be biased and the role of model sensitivity discrepancy in causing the projection difference may be exaggerated.

Forcing uncertainty, as reflected by the intermodel spread of the forcing, may be caused by the uncertainty in both the instantaneous forcing and the rapid adjustments. As for the instantaneous forcing, the uncertainty may be because of the inaccuracy of the radiation code used in different general circulation models (GCMs) (Collins et al. 2006) as well as the difference in atmospheric climatology in these models (Huang 2013a). As for the adjustments, while the stratospheric adjustment is essentially a radiative equilibration of the stratosphere and thus is likely better constrained, the tropospheric component may vary as much as the long-term feedbacks (Andrews and Forster 2008; Gregory and Webb 2008).

In summary, it is important to properly quantify the overall radiative forcing and understand the sources of its uncertainty in analyzing climate feedback and sensitivity and attributing model projection difference. However, the forcing values are not routinely archived together with other fields in the model intercomparison programs. In practice, radiative forcing can be measured

Corresponding author address: Dr. Yi Huang, Dept. of Atmospheric and Oceanic Sciences, McGill University, 805 Sherbrooke Street West, Montreal, QC H3A 0B9, Canada.
E-mail: yi.huang@mcgill.ca

DOI: 10.1175/JCLI-D-13-00535.1

by a partial radiative perturbation technique (PRP; Wetherald and Manabe 1988), a linear regression method (Gregory 2004), or a radiative kernel-based total radiation change decomposition method (Huang 2013a). The PRP method is accurate, but computationally expensive; the regression method is inexpensive, but can only be applied to time-invariant forcing and cannot separate the instantaneous forcing from the adjustments; and the third method is also inexpensive, evaluates each forcing component, and can be applied to time-variant forcing. In this study, we use this third method proposed by Huang (2013a) to explicitly assess all the components of the radiative forcing in each model in phase 5 of the Coupled Model Intercomparison Project (CMIP5) abrupt quadrupling of atmospheric CO_2 experiments abrupt4×CO_2 and sstClim4×CO_2 (Taylor et al. 2012). In the following sections, we will explain the method, measure the uncertainty in our forcing estimation in the idealized experiments, compare our results with those of the other two methods, and discuss the effects of forcing uncertainty on analyzed climate sensitivity and feedback.

2. Methodology

a. Analysis procedure

In this study, we use the method proposed by Huang (2013a) to estimate the radiative forcing in each model. This method is based on the decomposition of the overall change in the TOA radiation flux ΔR. Following a Taylor expansion, we have

$$\Delta R = F_i + \sum\left(\frac{\partial R}{\partial X}\Delta X\right) + Z, \tag{1}$$

where F_i denotes instantaneous forcing resulting from quadrupling CO_2; Z denotes the residual; and X denotes a physical quantity that influences R, including surface, tropospheric, and stratospheric temperature (T_S, $T_{\rm tr}$, and $T_{\rm st}$, respectively), tropospheric and stratospheric water vapor ($W_{\rm tr}$ and $W_{\rm st}$, respectively), surface albedo A, and clouds C. The contribution of a climate variable change ΔX to the change in R is referred to as a ''radiative response'' (for brevity, response is used hereafter) and denoted as ΔR_X. Here, a noncloud response is assessed by the kernel method (Huang et al. 2007b; Soden et al. 2008; Shell et al. 2008):

$$\Delta R_X = \frac{\partial R}{\partial X}\Delta X, \tag{2}$$

where $\partial R/\partial X$ is a precalculated radiative sensitivity kernel. The total response ΔX can be conceptually partitioned to feedback (arising from T_S change) and forcing adjustment (unrelated to T_S). To distinguish them we denote the adjustment with a superscripted asterisk. For example, the stratosphere-adjusted forcing consists of F_i and the stratospheric contributions unrelated to T_S:

$$F_a = F_i + \Delta R^*_{T_{\rm st}} + \Delta R^*_{W_{\rm st}}. \tag{3}$$

Note that the forcing and adjustment in this paper are analyzed using the radiation fluxes at the TOA instead of the tropopause. However, it can be shown that after the stratosphere equilibrates, the stratosphere-adjusted forcing F_a is identical at the two levels. Andrews and Forster (2008) and Gregory and Webb (2008) also consider a portion of tropospheric responses that do not directly result from globally averaged T_S variation as an adjustment to the radiative forcing. We denote the fully adjusted forcing including the tropospheric adjustment F^*_a:

$$F^*_a = F_a + \sum\Delta R^*_{X_{\rm tr}}. \tag{4}$$

Here $X_{\rm tr}$ may include tropospheric adjustments in temperature, water vapor, cloud, surface albedo, and so on.

The overall change in the clear-sky outgoing longwave radiation (OLR) can be decomposed into seven terms:

$$\Delta R^{\rm clr} = F^{\rm clr}_i + \Delta R^{\rm clr}_{T_S} + \Delta R^{\rm clr}_{T_{\rm tr}} + \Delta R^{\rm clr}_{W_{\rm tr}} + \Delta R^{\rm clr}_{T_{\rm st}} + \Delta R^{\rm clr}_{W_{\rm st}} + Z^{\rm clr}. \tag{5}$$

If $Z^{\rm clr}$ is small (Huang 2013a), one can first estimate the clear-sky instantaneous forcing $F^{\rm clr}_i$ by subtracting from model-simulated total change $\Delta R^{\rm clr}$ the noncloud responses $\Delta R^{\rm clr}_X$ quantified through the kernel method. The clear-sky stratosphere-adjusted forcing $F^{\rm clr}_a$ can be obtained by combining $F^{\rm clr}_i$ with stratospheric adjustment [Eq. (3)]. Then, the all-sky stratosphere-adjusted forcing F_a can be obtained using an empirical ratio (Soden et al. 2008): $F^{\rm clr}_a/F_a = 1.16$. Subtracting from F_a the all-sky stratospheric contributions obtained, again, by using the kernel method renders the all-sky instantaneous forcing F_i.

Note that the difference between the clear-sky and all-sky radiative forcing is caused by the cloud-masking effect, which can be measured by cloud forcing (CF; the difference between R and $R^{\rm clr}$). In recognition of this, we further apply a CF scaling to relate F_a to $F^{\rm clr}_a$:

$$\frac{F^{\rm clr}_a - F_a}{(F^{\rm clr}_a)_{\rm ref}} = \frac{0.16}{1.16}\frac{\rm CF}{({\rm CF})_{\rm ref}}. \tag{6}$$

In this study, we take the reference clear-sky forcing $(F^{\rm clr}_a)_{\rm ref}$ and cloud forcing $({\rm CF})_{\rm ref}$ as the multimodel

ensemble mean (MME) of the long-term global mean of these quantities. Then, F_a in each grid box of each model can be estimated [see further discussion of Eq. (6) in the appendix]. The all-sky instantaneous forcing F_i is then obtained by subtracting the all-sky stratospheric adjustment from F_a [see Eq. (3)].

Finally, to complete the analysis, the cloud response, either classified as forcing adjustment or feedback, is estimated as

$$\Delta R_C = \Delta R - F_i - \sum \Delta R_X . \tag{7}$$

Given the forcing F_i estimated as above, this is equivalent to using the cloud-forcing adjustment method (Soden et al. 2008; Shell et al. 2008) with explicitly assessed radiative forcing. Note that $\sum \Delta R_X$ here includes the contributions from feedback, as well as stratospheric and tropospheric adjustments.

Although the CO_2 forcing is mostly exerted on the longwave radiation, the above procedure can be used for estimating the forcing and feedback in longwave (LW) and shortwave (SW) radiation separately. Substituting the noncloud responses, forcing and cloud response obtained using Eqs. (2), (6), and (7), respectively, back to Eq. (1), we may obtain a nonzero Z, which measures the overall error in the decomposition of the radiation energy budget change.

Based on the linear relationship noticed between globally averaged radiation and surface temperature variations, a climate sensitivity parameter can be derived as

$$S^{-1} = \frac{\langle \Delta R - F_a^* \rangle}{\langle \Delta T_s \rangle}, \tag{8}$$

where $\langle\ \rangle$ denote the global average. From Eq. (1), were the residual zero, the sensitivity parameter would be equal to the sum of all the feedback parameters:

$$S^{-1} = \sum \lambda_X . \tag{9}$$

Here each feedback parameter $\lambda_X = \langle \Delta R_X \rangle / \langle \Delta T_s \rangle$. Similarly, the residual $Z^\lambda = \langle Z \rangle / \langle \Delta T_s \rangle$ quantifies the accuracy of the climate sensitivity parameter estimation.

b. Data

We analyze the radiative forcing, feedback, and sensitivity in the CMIP5 GCMs using the data from four experiments: the preindustrial fully coupled control run (piControl), abrupt4×CO_2 (as in piControl but run for 150 yr after instantaneous quadrupling of atmospheric CO_2, then holding it fixed), sstClim [as in piControl but run for 30 yr with the climatological sea surface temperature (SST) and sea ice derived from the piControl run] and sstClim4×CO_2 (as in sstClim but with atmospheric levels of CO_2 instantaneously quadrupled and then held fixed). The details of these experiments are documented by Taylor et al. (2012). Differences between the abrupt4×CO_2 (sstClim4×CO_2) and the 30-yr climatology of piControl (sstClim) experiments are calculated as the climate responses to the quadrupling of atmospheric CO_2.

Figures 1 and 2 summarize the climate responses of atmospheric temperature and humidity in the 11 GCMs at the end of the abrupt4×CO_2 experiment. The quadrupling of CO_2 causes dramatic changes in the atmospheric states. The tropospheric temperature and specific humidity generally increase in the models with maximum changes occurring in the tropical upper troposphere (up to 15-K warming and 4 times increase in specific humidity), which tend to maintain the relative humidity. In the stratosphere, however, specific humidity increases despite the strong (up to 15 K) cooling. There are large model discrepancies in the magnitude and pattern of the stratospheric water vapor change, which leads to quantitatively different radiative feedbacks from them.

We apply two sets of kernels previously created from the Community Atmosphere Model, version 3 (CAM3), of the National Center for Atmospheric Research (NCAR; Shell et al. 2008) at 2.8° × 2.8° resolution, and the Atmospheric Model, version 2 (AM2), of the Geophysical Fluid Dynamics Laboratory (GFDL; Soden et al. 2008) at 2.5° × 2° resolution to calculate the feedbacks. Like Vial et al. (2013), we find the noncloud feedbacks computed from the two sets of kernels in very good agreement with each other (the difference in global means is generally less than 10% and is much less than the intermodel feedback difference obtained using either set of the kernels). Because the AM2 kernels are of higher horizontal resolution but do not include the upper stratosphere, our presentation and discussion is focused on the analysis results based on the tropospheric feedbacks computed from the AM2 kernels and the stratospheric feedbacks computed from the CAM3 kernels.

To obtain tropospheric climate feedbacks, the temperature and water vapor contributions are vertically integrated from surface to the tropopause; for stratospheric feedbacks the integration is done from the tropopause to 10 hPa. Noticing the delicate temperature and water vapor changes near the tropopause (see Figs. 1, 2), we compute the tropopause level as the lowest level where the temperature lapse rate is less than 2 K km^{-1} for a depth of more than 2 km in each grid box in each model following the standard definition of the World Meteorological Organization (WMO 1957), instead of using the linear interpolation

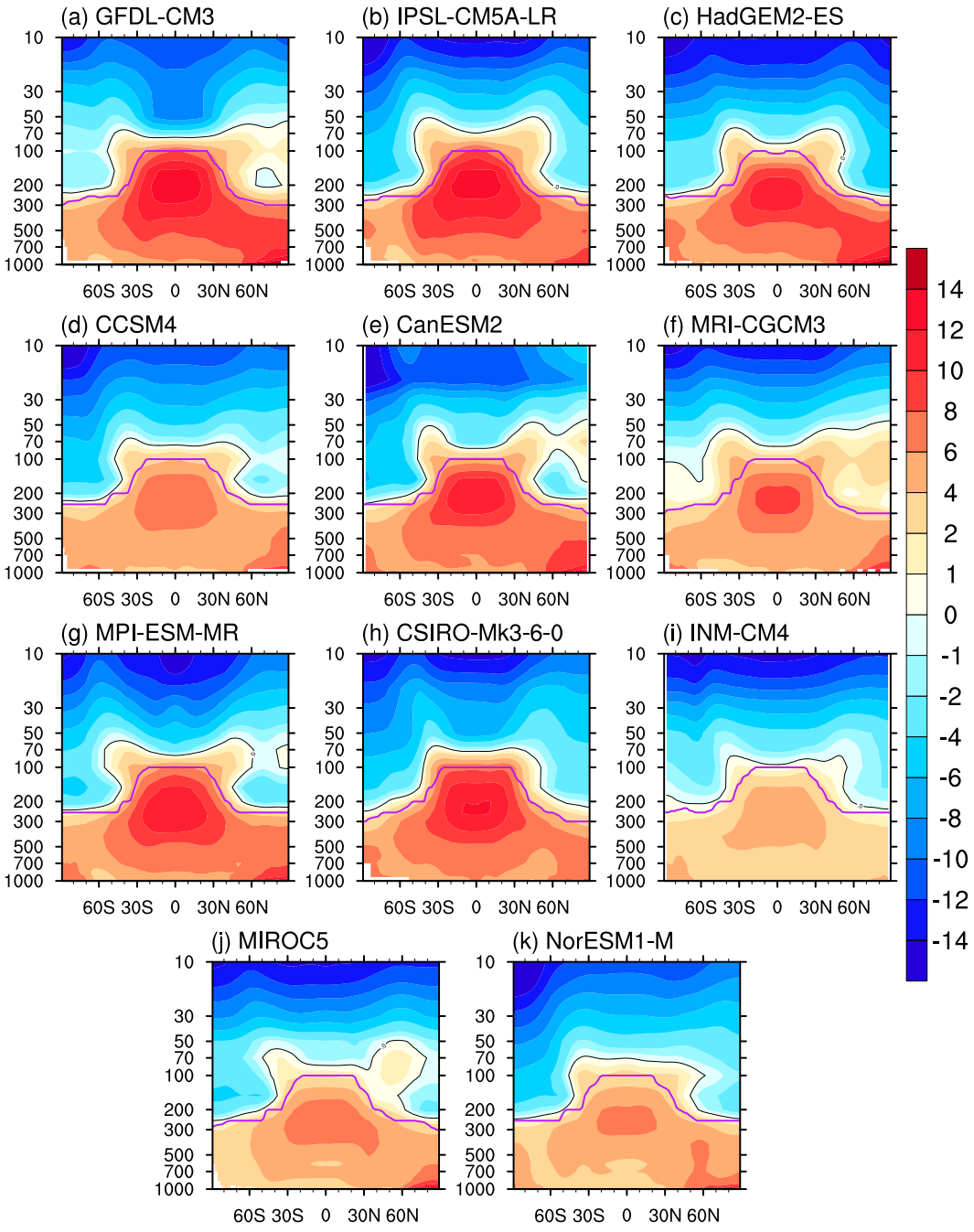

FIG. 1. Zonal-mean atmospheric temperature change (shading) by the end of the abrupt4×CO_2 experiment. The black (purple) line marks zero temperature change (the lapse-rate tropopause).

method adopted in other studies (e.g., Soden et al. 2008; Shell et al. 2008).

The global-mean noncloud feedbacks ΔR_X, together with the forcing and cloud feedback (detailed in the following sections), from the 11 models are presented in Tables 1and 2 (along with a complete list of all model expansions in Table 1).

3. Results

a. *Global-mean forcing*

Following the procedure outlined in section 2, we diagnose the global-mean forcing in the abrupt4×CO_2 experiment. First, the clear-sky instantaneous forcing F_i^{clr} is estimated using Eq. (5), through decomposing the

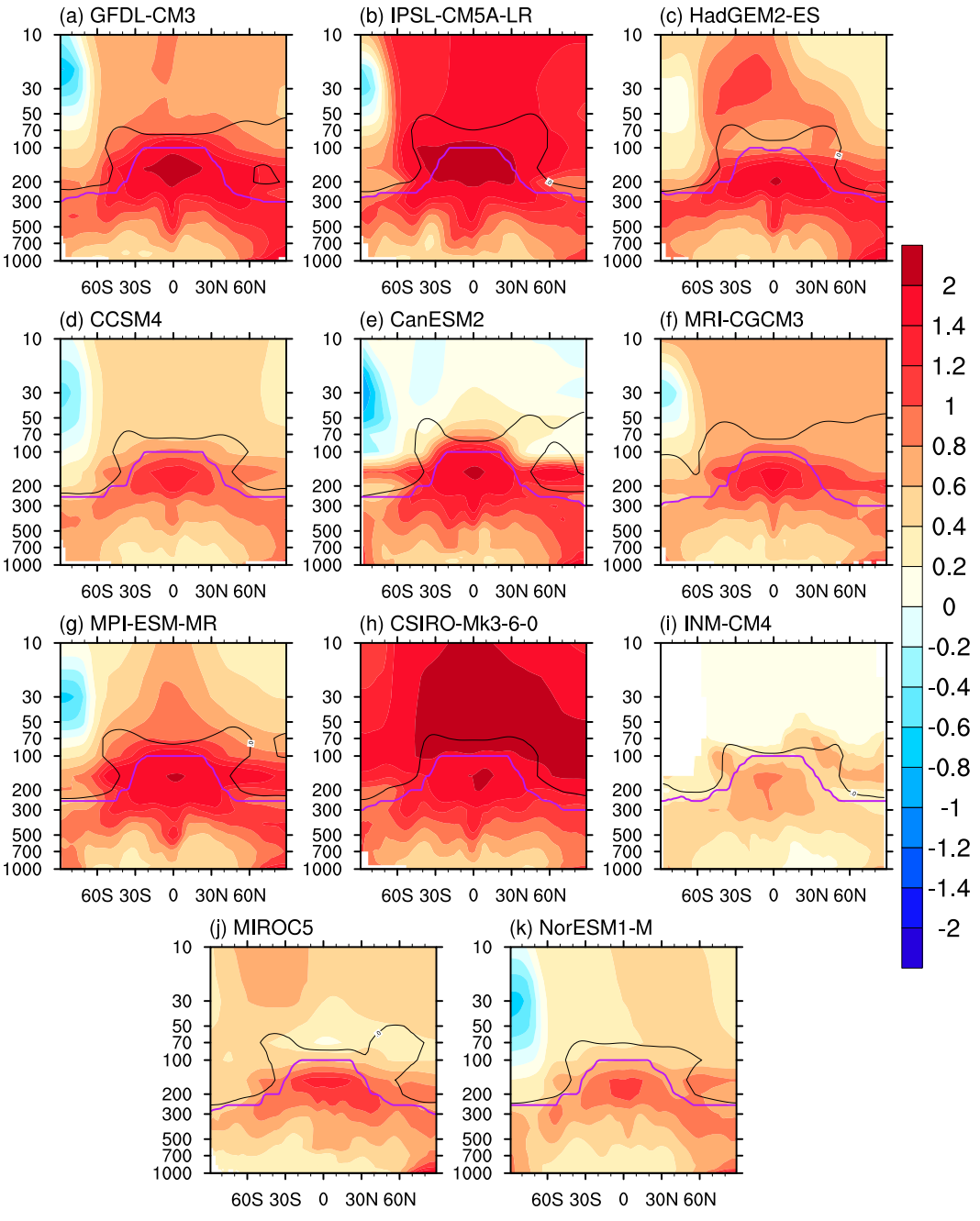

FIG. 2. As in Fig. 1, but for the binary logarithm of water vapor change $\Delta[\log_2(q)]$.

total radiation change in relevance to the climatology of piControl. To minimize the nonlinearity effect (Z^{clr}) in the estimation, we calculate F_i^{clr} in the first year of the 150-yr integration when the climate response is the smallest in magnitude. The stratospheric adjustment is calculated by multiplying the stratospheric temperature and water vapor responses with the kernels, assuming all the stratospheric responses in the first year are completely radiative adjusted (unrelated to globally averaged T_S, which has had little change). Then, the all-sky forcing is obtained using Eq. (6).

Our estimations of the multimodel-mean, all- and clear-sky, stratosphere-adjusted forcings are 7.29 and 8.46 W m^{-2}, respectively (see Table 1 for the all-sky values of each model), about 3% lower than the estimation of Vial et al. (2013) (7.545 and 8.785 W m^{-2}, respectively; J. Vial et al. 2013, personal communication), which are obtained using the PRP method from

TABLE 1. Decomposition of ΔR. Radiative forcing components (W m^{-2}). Instantaneous forcing (F_i) and stratospheric adjustment ($\Delta R^*_{\rm st}$, with components $\Delta R^*_{T_{\rm st}}$ and $\Delta R^*_{W_{\rm st}}$) are derived from the abrupt4×CO_2 experiment, while the tropospheric adjustment ($\Delta R^*_{\rm tr}$, with components $\Delta R^*_{T_{\rm tr}}$, $\Delta R^*_{W_{\rm tr}}$, and $\Delta R^*_{\tilde{C}}$) is from the sstClim4×CO_2 experiment. The sum of the first two terms is the stratosphere-adjusted forcing (F_a) and the sum of the three terms is the fully adjusted forcing (F^*_a). The last two columns show the fully adjusted forcing (LW and total) obtained using the linear regression method (Andrews et al. 2012) for comparison.

		Stratospheric adjustment				Tropospheric adjustment (fixed SST)								
		LW				LW				LW + SW	F^*_a		F^*_a (regression)	
Models	F_i	$\Delta R^*_{T_{\rm st}}$	$\Delta R^*_{W_{\rm st}}$	$\Delta R^*_{\rm st}$	F_a	$\Delta R^*_{T_{\rm tr}}$	$\Delta R^*_{W_{\rm tr}}$	$\Delta R^*_{\tilde{C}}$	$\Delta R^*_{\rm tr}$	$\Delta R^*_{\rm tr}$	LW	LW + SW	LW	LW + SW
Geophysical Fluid Dynamics Laboratory Climate Model, version 3 (GFDL CM3)	4.90	1.76	0.04	1.80	6.70	−1.67	0.63	−0.32	−1.36	0.66	5.35	7.37	5.66	5.89
L'Institut Pierre-Simon Laplace Coupled Model, version 5, coupled with Nucleus for European Modelling of the Ocean (NEMO), low resolution (IPSL-CM5A-LR)	4.51	1.55	0.05	1.60	6.10	−1.84	0.54	−1.55	−2.85	0.19	3.25	6.29	3.16	6.17
Hadley Centre Global Environment Model, version 2–Earth System (HadGEM2-ES)	5.55	2.16	0.03	2.19	7.74	−1.63	0.26	−0.33	−1.70	−0.56	6.04	7.18	5.89	5.76
Community Climate System Model, version 4 (CCSM4)	5.51	1.82	0.01	1.83	7.34	−2.00	0.37	−0.07	−1.71	0.28	5.64	7.62	4.63	5.07
Second Generation Canadian Earth System Model (CanESM2)	5.74	1.72	0.01	1.73	7.47	−1.80	0.37	−0.09	−1.52	0.02	5.96	7.50	5.96	7.46
Meteorological Research Institute Coupled Atmosphere–Ocean General Circulation Model, version 3 (MRI CGCM3)	5.23	1.89	0.04	1.93	7.16	−1.39	0.40	−0.14	−1.13	0.09	6.03	7.25	6.23	6.43
Max Planck Institute Earth System Model, medium resolution (MPI-ESM-MR)	6.12	1.93	0.03	1.96	8.08	−1.68	0.39	−0.22	−1.51	0.55	6.57	8.63	6.54	8.06
Commonwealth Scientific and Industrial Research Organisation Mark, version 3.6.0 (CSIRO Mk3.6.0)	5.75	1.77	0.02	1.78	7.54	−1.27	0.30	−0.90	−1.88	−1.24	5.66	6.30	6.17	5.10
Institute of Numerical Mathematics Coupled Model, version 4.0 (INM CM4)	5.01	2.07	0.01	2.08	7.08	−1.58	0.50	0.32	−0.76	−0.87	6.33	6.22	6.76	5.81
Model for Interdisciplinary Research on Climate, version 5 (MIROC5)	5.62	2.03	0.02	2.04	7.66	−1.56	0.29	−0.61	−1.87	−0.07	5.79	7.59	6.32	8.18
Norwegian Climate Centre Earth System Model, version 1 (intermediate resolution) (NorESM1-M)	5.55	1.76	0.01	1.77	7.32	−1.84	0.35	−0.54	−2.03	−0.29	5.29	7.03	5.69	6.10
MME	5.41	1.86	0.02	1.88	7.29	−1.66	0.40	−0.40	−1.66	−0.11	5.63	7.18	5.73	6.37
STD	0.46	0.18	0.01	0.17	0.54	0.21	0.11	0.5	0.54	0.58	0.88	0.72	1.02	1.08

TABLE 2. As in Table 1, but for climate feedback components ($W m^{-2}$). The term ΔR is the total radiative flux change, and ΔR_X is the climate feedback, which does not include the tropospheric adjustment (see text). Some values for the CSIRO Mk3.6.0 model are missing for lack of shortwave surface radiation data needed by albedo calculation.

	All-sky LW								All-sky SW					SW + LW	
		Tropospheric feedback			Stratospheric feedback										
Models	ΔR	$\Delta R_{T_{tr}}$	$\Delta R_{W_{tr}}$	ΔR_C	$\Delta R_{T_{st}}$ $(dT > 0)$	$\Delta R_{T_{st}}$ $(dT < 0)$	$\Delta R_{W_{st}}$	Z	ΔR	ΔR_A	ΔR_W	ΔR_C	Z	ΔR_{net}	Z
GFDL CM3	−6.11	−22.50	8.58	2.36	−0.15	0.09	0.13	0.02	7.59	1.79	1.72	2.45	−0.04	1.48	−0.38
IPSL-CM5A-LR	−7.97	−22.46	9.47	2.40	−0.04	0.35	0.10	−1.05	9.90	0.98	1.79	4.29	−0.20	1.93	−1.25
HadGEM2-ES	−4.10	−22.62	8.90	3.23	−0.07	0.22	0.10	0.10	5.88	2.11	1.80	0.14	0.67	1.78	0.78
CCSM4	−4.60	−15.50	5.89	−0.42	−0.05	0.01	0.03	−0.29	3.81	1.80	1.23	−1.18	−0.02	−0.79	−0.31
CanESM2	−2.41	−21.24	8.72	4.51	−0.06	0.03	0.15	−0.46	3.89	1.73	1.70	−1.10	0.01	1.48	−0.45
MRI CGCM3	−3.53	−15.65	5.90	0.27	−0.17	−0.08	0.10	0.06	4.52	1.44	1.17	0.75	−0.07	0.99	−0.01
MPI-ESM-MR	−3.18	−21.26	8.45	2.70	−0.10	0.26	0.11	0.01	4.74	1.52	1.62	−0.18	−0.29	1.56	−0.19
CSIRO Mk3.6.0	−4.75	−21.40	8.63	1.73	−0.07	0.36	0.02	0.32	6.60	—	1.64	—	—	1.85	—
INM-CM4	0.83	−10.02	3.94	0.91	−0.02	0.05	0.04	−0.40	0.61	0.86	0.76	−0.64	−0.26	1.45	−0.67
MIROC5	−1.73	−14.91	6.00	1.59	−0.05	0.06	0.05	−0.25	3.53	1.30	1.21	−1.18	0.39	1.80	0.14
NorESM1-M	−1.77	−13.44	5.08	1.40	−0.04	0.09	0.03	−0.19	3.45	1.11	1.06	−0.49	0.02	1.68	−0.16
MME	−3.57	−18.27	7.23	1.88	−0.07	0.14	0.08	−0.18	4.96	1.46	1.43	0.29	−0.01	1.38	−0.25
STD	2.37	4.46	1.90	1.38	0.05	0.14	0.05	0.38	2.47	0.40	0.35	1.79	0.33	0.77	0.53

the atmosphere and radiation code of the Laboratoire de Météorologie Dynamique zoom (LMDZ) GCM. As the CO_2 perturbation is identically prescribed in the sstClim4×CO_2 and abrupt4×CO_2 experiments, we also validate the longwave forcing components analyzed from the two experiments against each other (Figs. 3a–c). The correlation coefficient between the two sets of all-sky stratosphere-adjusted forcing is 0.77 (0.93 if excluding CCSM4) and the root-mean-square (RMS) difference is 0.40 $W m^{-2}$ (about 5% of the mean). This agreement confirms the accuracy of the stratosphere-adjusted forcing estimation and also suggests that the forcing can be accurately diagnosed in transient climate change (as done for the abrupt4×CO_2 experiment) without relying on auxiliary experiments (such as the sstClim4×CO_2 experiment). We suspect the bigger difference in CCSM4 arises from inconsistent configuration of the experiment of this model (the metadata in the CCSM4 data file indicates that the sstClim4×CO_2 experiment is forced by observed SST and multiple forcing species, as opposed to the preindustrial climatologic SST and CO_2-only forcing used by the other models).

As the forcing does not vary with time in the 4×CO_2 experiment, the fully adjusted forcing (after both tropospheric and stratospheric adjustments) can also be obtained using the linear regression method (Andrews et al. 2012). To validate against this forcing estimate, we use the aid of the sstClim4×CO_2 experiment, in which the feedback is shut off by design, to obtain the tropospheric adjustment. The adjustment is calculated by multiplying the kernels with the responses computed as the difference between the sstClim4×CO_2 and sstClim experiments. The global-mean overall tropospheric adjustment is found to be very small (ensemble mean: −0.11 $W m^{-2}$), which results from the compensation of various adjustment components; this is in agreement with Vial et al. (2013). As shown in Fig. 3d and Table 1, we find that the all-sky fully adjusted longwave forcing obtained by the two methods agree very well with each other. The correlation coefficient between the two sets of forcing estimates is 0.90; the RMS difference is 0.43 $W m^{-2}$ (~8%). The discrepancy in the shortwave is greater (see Table 1, using the total minus longwave), which may have resulted from the different adjustment (especially that of clouds) in the sstClim4×CO_2 experiment as compared to the abrupt4×CO_2 experiment (Andrews et al. 2012), the imperfect isolation of the nonfeedback effect from the feedback effect using the regression method, and the uncertainties in F_i and ΔR_{st}^* estimations here.

Last, the residual [Z in Eq. (1)] in the decomposition of the total radiation change ΔR in the years following the first year in the abrupt4×CO_2 experiment provides another assessment of the accuracy of our forcing estimation. Figure 4 shows how the total longwave radiation varies with time and how various components contribute to its change. It is clear that as the response ΔX becomes large, so does the residual Z. This residual would be the bias in the forcing if it were estimated in the following years (instead of the first year). This bias is mainly due to the nonlinearity effect in the radiative response (ΔR_X) estimation using only the linear kernels. Nevertheless, even in the end years (see Table 1), that is, under a worst-case scenario, Z is about 3% of F_i on average (23% in the worst case for the IPSL-CM5A-LR model).

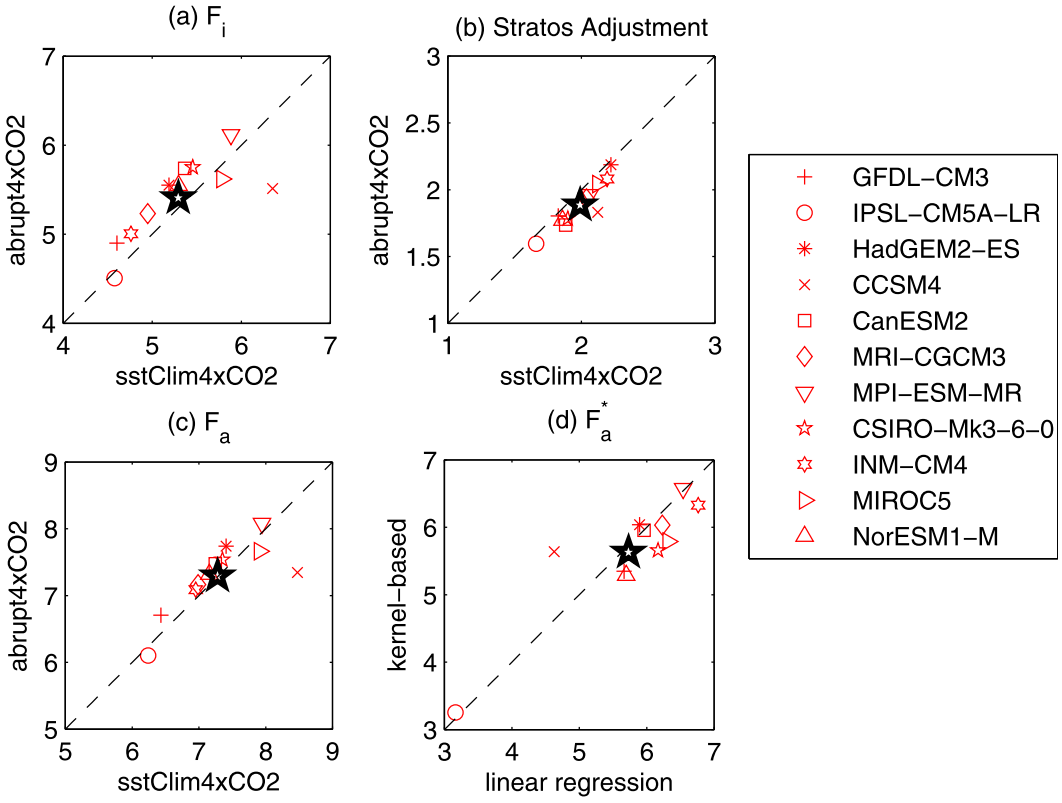

FIG. 3. Estimated global-mean all-sky longwave forcing. (a) Instantaneous forcing, (b) stratospheric adjustment, and (c) stratosphere-adjusted forcing of each model derived from the abrupt4×CO_2 (y axis) experiment vs those from the sstClim4×CO_2 (x axis) experiment. (d) Fully adjusted forcing derived following the method presented in this paper (y axis) vs those obtained using the linear regression method (x axis) (Andrews et al. 2012). Different markers represent individual models, and the black star donates the MME.

In summary, the multimodel-mean, all-sky, fully adjusted forcing is 7.18 W m^{-2}, which consists of 5.41 W m^{-2} instantaneous forcing, 1.9 W m^{-2} stratospheric adjustment, and −0.11 W m^{-2} tropospheric adjustment. There is substantial intermodel variation in the radiative forcing: an intermodel standard deviation (STD) of 0.71 W m^{-2} (about 10% of the mean) and a maximum–minimum range of 2.41 W m^{-2} (about 34%). We find that the uncertainties in instantaneous forcing, stratosphere adjustment, and the tropospheric adjustment have an intermodel STD of 0.46, 0.17, and 0.58 W m^{-2}, respectively. No pair of the three components has a statistically significant correlation. This indicates that all the forcing components contribute to the overall uncertainty in the fully adjusted radiative forcing and thus reaffirms that all of them need to be properly assessed in the feedback analysis.

b. *Geographic distribution of the forcing*

Figure 5 shows the multimodel mean and intermodel variation of the spatial distribution of the three forcing components: instantaneous forcing, stratospheric adjustment, and tropospheric adjustment. Although the CO_2 concentration and perturbation are uniformly prescribed, it is clear from Fig. 5a that the instantaneous forcing has a geographically nonuniform distribution. The forcing generally decreases from low to high latitudes because of the Planck effect (less emission at lower temperatures and thus less greenhouse effect); the abundant clouds and water vapor in the deep convective regions (the ITCZ) in the tropics result in local minima of the forcing due to their masking effect. The greatest intermodel discrepancies exist on the edges of the ITCZ regions, which reflect the discrepancies in the location and area of the ITCZ among these models.

In comparison, the stratospheric adjustment is much more uniform. It is generally positive as it mainly results from the radiative cooling of the stratosphere induced by CO_2 perturbation. The zonally asymmetric pattern in the high latitudes in both hemispheres is a result of the asymmetric temperature responses there.

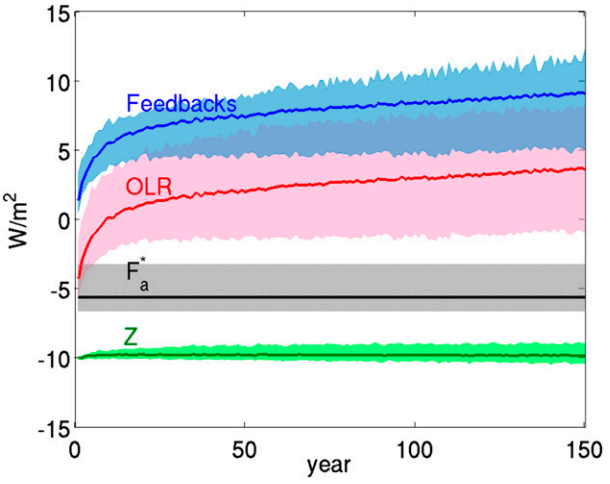

FIG. 4. Variation of the longwave radiation in each model. The solid lines (shading) represent the multiple model mean (spread) of total longwave radiation change (red), the sum of longwave climate feedbacks (blue), the fully adjusted forcing (black), and residuals (offset by −10, green), respectively.

Although the global mean of the tropospheric adjustment is dominated by the temperature adjustment (see Table 1), as shown by Vial et al. (2013), the considerable geographic variations mainly result from cloud adjustment, which has a great intermodel STD.

c. *Climate sensitivity and feedback*

When forcing is explicitly estimated as done in the previous section, the residual Z^{λ} on average is $-0.06\,\mathrm{W\,m^{-2}\,K^{-1}}$ (see Table 3), about 4% of the mean climate sensitivity parameter, with longwave and shortwave contributions being -0.05 and $-0.01\,\mathrm{W\,m^{-2}\,K^{-1}}$, respectively. In the worst case (for the IPSL-CM5A-LR model), the residual is about 36% of the overall sensitivity parameter. The residuals are generally less than what would be obtained when a constant stratosphere-adjusted forcing is prescribed in the analysis (e.g., in Vial et al. 2013), which indicates forcing estimation improves the performance of the linear decomposition of the climate sensitivity.

Applying perturbation analysis to Eq. (8), we can obtain an error budget of surface temperature change

$$\delta(\Delta T_s) = \frac{\delta(\Delta R - F_a^*)}{(S^{-1})_m} - (\Delta T_s)_m \frac{\delta(S^{-1})}{S^{-1}}. \qquad (10)$$

Here, the subscript m denotes the true value, which can be estimated by multimodel mean; δ denotes the error, which can be estimated by intermodel STD. Using the data presented in Tables 1–3, the two terms on the right-hand side are estimated to be roughly 1.0 and 1.3 K, respectively (note they are not uncorrelated). As the STD of ΔR and F_a^* are about equal, the uncertainty in the first term can be considered equally resulting from the two components. This indicates that about one-fourth of the overall ΔT_s uncertainty can be attributed to the forcing uncertainty. This is in agreement with Geoffroy et al. (2012) and Webb et al. (2013), who estimate the contribution using a different approach.

The noncloud feedbacks are computed by multiplying the kernels with responses and thus are not affected by the forcing estimation. It is interesting that we find the magnitudes of these feedbacks are insensitive to whether we separate the tropospheric adjustment from the overall tropospheric response in the analysis (not shown).

The cloud feedback as estimated from Eq. (7) is dependent on the forcing estimation. If the forcing is not explicitly estimated but assumed to be a constant value in all the models, the cloud feedback is found to be slightly biased (not shown), which is consistent with what Huang (2013a) finds.

Last, we find that a portion of the stratospheric effect varies with time because of continued cooling and moistening in the stratosphere (Table 3). It is important to realize that the stratospheric effect can be more than an adjustment of the forcing because the time-variant components may be linked to surface temperature change, which then constitutes a feedback mechanism (Huang 2013a,b). Here, we find in this $4 \times CO_2$ experiment that the radiative impact of this time-variant stratospheric effect is of much smaller magnitude than the initial stratospheric adjustment (9% on average and 27% in the extreme case). It is interesting to note, however, that above the tropopause level determined as described in section 2, stratospheric temperature changes are not uniform. The lowermost portion of the stratosphere warms in contrast to the radiatively cooled upper portions. This warming in some models extends to higher than 70 hPa and beyond 45° latitude (Fig. 1). The overall time-variant stratospheric temperature effect thus comprises compensating contributions from within the stratosphere.

4. Conclusions

In this study, we use a procedure proposed by Huang (2013a) to dissect the radiative forcing in the CMIP5 abrupt4×CO_2 experiment. Multiple validation tests show that the errors in our forcing estimates are generally within 10%. Our results show that quadrupling CO_2 induces an instantaneous all-sky forcing of $5.4\,\mathrm{W\,m^{-2}}$ on

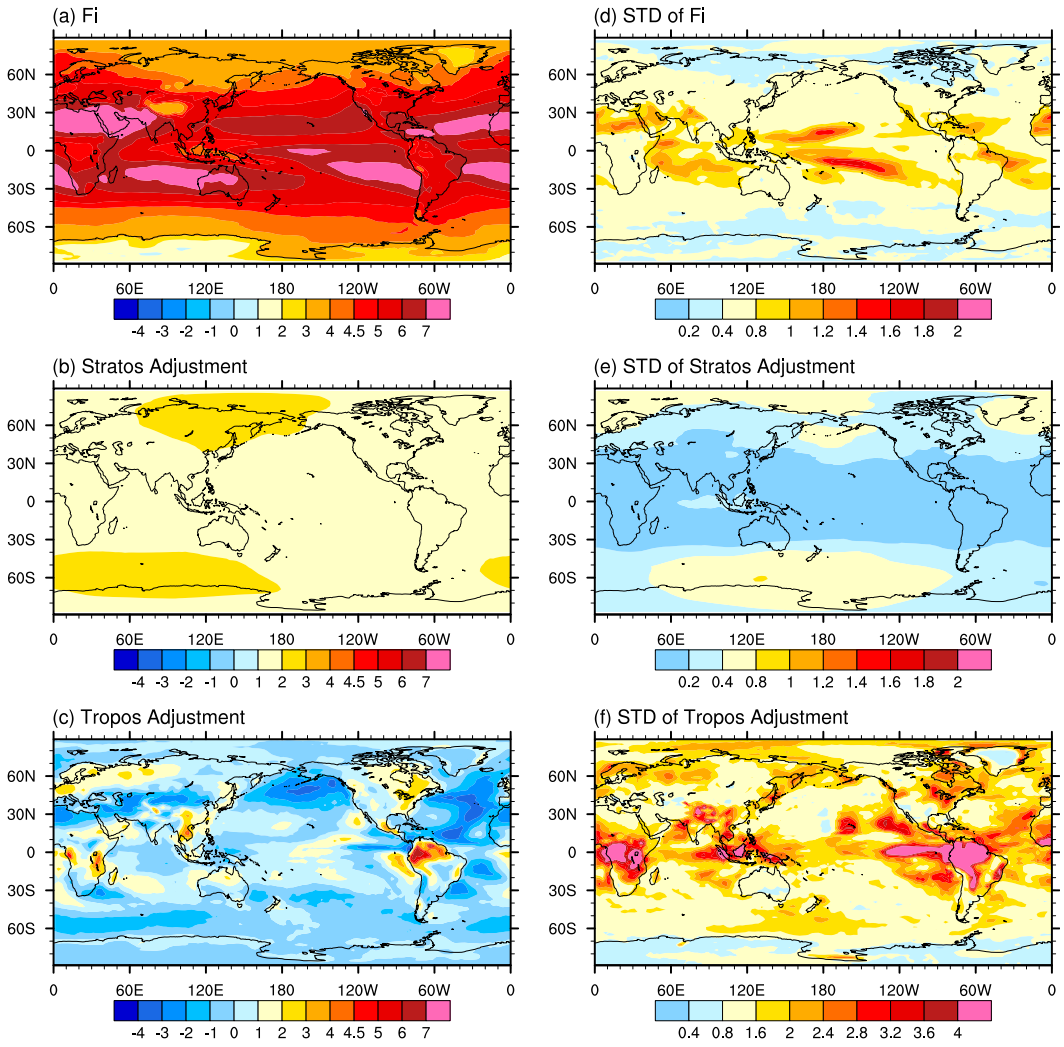

FIG. 5. Geographic distribution of the forcing component. MME of (a) instantaneous forcing, (b) stratospheric adjustment, and (c) tropospheric adjustment. (d)–(f) As in (a)–(c), but for the intermodel STD.

average, which is amended by a stratospheric adjustment of $1.9\,\mathrm{W\,m^{-2}}$ and a tropospheric adjustment of $-0.11\,\mathrm{W\,m^{-2}}$. The resulting fully adjusted overall forcing has an ensemble mean of $7.2\,\mathrm{W\,m^{-2}}$ and a substantial intermodel spread. The uncertainty in the overall forcing as reflected by this spread results from all the forcing components, especially the instantaneous forcing and tropospheric adjustment. These results reaffirm the importance of evaluating the radiative forcing components in climate feedback analyses.

It is worth noting that the analysis method presented here does not require either the forcing or climate sensitivity to be constant or to be known beforehand and thus can be applied to analyzing the forcing in transient climate change with time-variant forcing, such as the observational records. Given the short radiative relaxation time in the stratosphere and assuming a small stratospheric feedback, one can determine the instantaneous forcing and stratospheric adjustment following the procedure presented and validated above. To determine the tropospheric adjustment, one still needs to partition the tropospheric changes or independently determine the fully adjusted forcing.

With model-dependent radiative forcing being explicitly estimated, the fidelity of the linear decomposition of the overall radiation variation and the decomposition of the climate sensitivity is noticeably improved. The analysis also affirms a significant contribution by forcing uncertainty to the surface temperature projection spread in the climate models, which is about half of the contribution of sensitivity uncertainty.

TABLE 3. Feedback and sensitivity parameters ($W m^{-2} K^{-1}$). Some values for the CSIRO Mk3.6.0 model are missing for lack of shortwave surface radiation data needed by albedo calculation.

Models	All-sky LW					All-sky LW					LW + SW	
	λ_T	λ_W	λ_C	λ_{T+W+C}	Z^λ	λ_A	λ_W	λ_C	λ_{A+W+C}	Z^λ	$\lambda_{T+W+A+C}$	Z^λ
GFDL CM3	−4.16	1.59	0.44	−2.14	0.00	0.33	0.32	0.45	1.10	−0.07	−1.03	−0.07
IPSL-CM5A-LR	−4.28	1.81	0.46	−2.02	−0.20	0.19	0.34	0.82	1.35	−0.04	−0.67	−0.24
HadGEM2-ES	−3.81	1.50	0.54	−1.77	0.02	0.36	0.30	0.02	0.68	0.11	−1.08	0.13
CCSM4	−3.58	1.36	−0.10	−2.31	−0.07	0.41	0.28	−0.27	0.43	−0.00	−1.88	−0.07
CanESM2	−3.84	1.58	0.81	−1.45	−0.08	0.31	0.31	−0.20	0.42	0.00	−1.03	−0.08
MRI CGCM3	−3.77	1.42	0.06	−2.28	0.02	0.35	0.28	0.18	0.81	−0.02	−1.47	−0.00
MPI-ESM-MR	−4.24	1.68	0.54	−2.02	0.02	0.30	0.32	−0.04	0.59	−0.06	−1.43	0.04
CSIRO Mk3.6.0	−4.00	1.61	0.32	−2.06	0.06	—	0.31	—	—	—	—	—
INM CM4	−3.96	1.59	0.36	−2.04	−0.16	0.34	0.30	−0.25	0.39	−0.10	−1.65	−0.26
MIROC5	−3.69	1.48	0.39	−1.81	−0.06	0.32	0.30	−0.29	0.33	0.10	−1.48	0.04
NorESM1-M	−3.69	1.39	0.38	−1.91	−0.05	0.31	0.29	−0.13	0.46	0.01	−1.45	−0.04
MME	−3.91	1.54	0.38	−1.98	−0.05	0.32	0.31	0.03	0.66	−0.01	−1.32	−0.06
STD	0.24	0.13	0.24	0.25	0.08	0.06	0.02	0.36	0.34	0.07	0.36	0.12

Acknowledgments. We thank Mark Zelinka, Andrew Dessler, Daniel Feldman, and two anonymous reviewers whose comments have greatly helped improve this paper. This work is supported by funding from the Natural Sciences and Engineering Research Council of Canada Discovery Program.

APPENDIX

Cloud-Forcing Scaling

Huang (2013a) discussed the accuracy of the clear-sky instantaneous forcing estimated using the decomposition method [Eq. (5)]. Here, we focus our discussion on the empirical ratio and the cloud forcing introduced in Eq. (6) in this paper.

Soden et al. (2008) first estimated an F^{clr}/F ratio of 1.16 using a GFDL GCM's atmosphere and radiation code. Vial et al. (2013) confirmed the value of this ratio based on the calculation using another GCM. As detailed below, our tests show that, although the ratio may vary, the variation of $F^{clr} - F$ can be very well predicted by cloud forcing.

Adopting the PRP method, we calculate the ''truth'' of the $4 \times CO_2$ instantaneous TOA longwave forcing using a radiation code moderate resolution atmospheric transmission (MODTRAN) and the present-day atmosphere simulated by a GFDL GCM [see Huang et al. (2007a) for the details regarding the configuration of the radiation calculation]. The unperturbed and perturbed CO_2 concentrations are prescribed uniformly across the globe to be 380 and 1520 ppm, respectively. Forcing at each model grid point in both clear-sky and all-sky conditions is calculated 3 hourly for 5 yr (nominal model years 2000–04). The 5-yr mean geographic distribution and the normalized global monthly-mean time series of the $4 \times CO_2$ forcing and CF are shown in Fig. A1. The 5-yr global mean of F^{clr} and F are 5.13 and 3.99 $W m^{-2}$, respectively. These values are noticeably less than the multimodel mean in the CMIP5 abrupt4×CO_2 experiment analyzed in the main text (see Table 1), although the distribution patterns are of great similarity. This is likely due to the difference in the atmospheric climatology (and thus the masking effect of water vapor, clouds, etc.) between the calculation here and the CMIP5 experiment.

Although the CO_2 concentration and its perturbation are prescribed to be constant values in the PRP calculations, there is considerable variation in the instantaneous forcing. The temporal variation in the global-mean forcing is about 10% of its mean value; the spatial variation is considerably larger.

Because the PRP calculation we conduct does not include the stratospheric adjustment (which varies from model to model), we examine the accuracy of Eq. (6) using just the instantaneous forcing (this renders a different value of the ratio, although our focus here is on its variability). We calculate the ratio between global monthly-mean F^{clr} and F that are shown in Fig. A1a. This ratio is remarkably stable with respect to the global mean in the month-to-month variation, with a mean of 1.29 and a standard deviation of about 1% of the mean. However, considerable spatial variation exists across the globe with a standard deviation in all the grid boxes exceeding 100% of the global-mean value. While the month-to-month variability of the global mean in 5 yr maybe underestimates the intermodel variability of the value, the pole-to-pole spatial variability should well exceed the intermodel variability.

Nevertheless, we find that even for the spatial variation, $F^{clr} - F$ can be well predicted by CF. The correlation

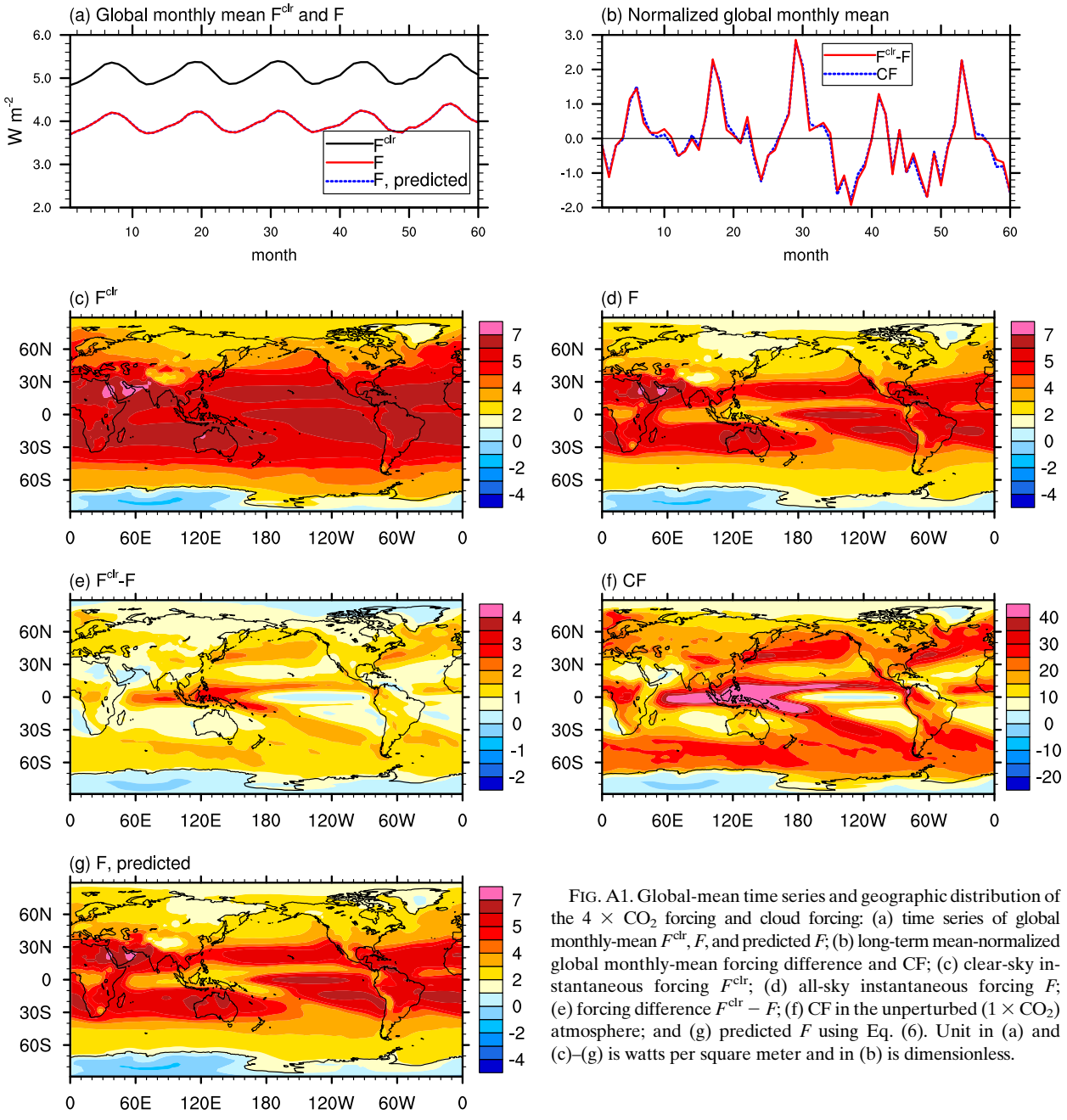

FIG. A1. Global-mean time series and geographic distribution of the 4 × CO_2 forcing and cloud forcing: (a) time series of global monthly-mean F^{clr}, F, and predicted F; (b) long-term mean-normalized global monthly-mean forcing difference and CF; (c) clear-sky instantaneous forcing F^{clr}; (d) all-sky instantaneous forcing F; (e) forcing difference $F^{clr} - F$; (f) CF in the unperturbed (1 × CO_2) atmosphere; and (g) predicted F using Eq. (6). Unit in (a) and (c)–(g) is watts per square meter and in (b) is dimensionless.

between $F^{clr} - F$ and CF is greater than 0.99 with respect to both month-to-month (Figure A1b) and geographic variations (Figs. A1e,f). We test how well F^{clr} and CF predict F according to Eq. (6). In our test, we set the reference clear-sky forcing $(F^{clr})_{ref}$ to be 5.13 W m^{-2} (the 5-yr global mean) and the reference CF to be 20.14 W m^{-2} (the 5-yr global mean CF of the unperturbed atmosphere). The results (cf. Figs. A1d,g and the red and blue lines in Fig. A1a) show the estimated F is in very good agreement with the truth with respect to both geographic distribution and global mean. The bias in estimated global-mean F is less than 0.001 W m^{-2} on average, with a RMS error of 0.003 W m^{-2}. The bias and RMS error in the global distribution of F are 0.001 and 0.05 W m^{-2}, respectively. Hence, we conclude that the CF scaling in Eq. (6) is capable of reducing the error in all-sky forcing estimation generally to less than 5%.

The CF scaling requires a reference CF value that pairs with the ratio in Eq. (6). As the main objective in this paper is to account for intermodel difference and

obtain geographic distribution of the forcing, we use the multimodel global-mean CF value from the control climate and assume it corresponds to the empirical ratio obtained by Soden et al. (2008) in our forcing assessment.

Although the CF-scaling method is assessed for the quadrupling CO_2 forcing here, a similar approach may be applied to other forcing types. However, it needs to be cautioned that because some forcing species (e.g., aerosols) have a much more inhomogeneous distribution than the well-mixed greenhouse gases, both geographically and vertically (in relevance to cloud height), the cloud-masking effect and thus the scaling ratio may be case dependent and subject to more uncertainty in other cases. Future work is required to validate the method in broader applications.

REFERENCES

Andrews, T., and P. M. Forster, 2008: CO_2 forcing induces semi-direct effects with consequences for climate feedback interpretations. *Geophys. Res. Lett.,* **35,** L04802, doi:10.1029/2007GL032273.

——, J. Gregory, M. Webb, and K. Taylor, 2012: Forcing, feedbacks and climate sensitivity in CMIP5 coupled atmosphere-ocean climate models. *Geophys. Res. Lett.,* **39,** L09712, doi:10.1029/2012GL051607.

Collins, W. D., and Coauthors, 2006: Radiative forcing by well-mixed greenhouse gases: Estimates from climate models in the Intergovernmental Panel on Climate Change (IPCC) Fourth Assessment Report (AR4). *J. Geophys. Res.,* **111,** D14317, doi:10.1029/2005JD006713.

Dufresne, J.-L., and S. Bony, 2008: An assessment of the primary sources of spread of global warming estimates from coupled atmosphere–ocean models. *J. Climate,* **21,** 5135–5144.

Forster, P. M., T. Andrews, P. Good, J. M. Gregory, L. S. Jackson, and M. Zelinka, 2013: Evaluating adjusted forcing and model spread for historical and future scenarios in the CMIP5 generation of climate models. *J. Geophys. Res.,* **118,** 1139–1150, doi:10.1002/jgrd.50174.

Geoffroy, O., D. Saint-Martin, and A. Ribes, 2012: Quantifying the sources of spread in climate change experiments. *Geophys. Res. Lett.,* **39,** L24703, doi:10.1029/2012GL054172.

Gregory, J. M., 2004: A new method for diagnosing radiative forcing and climate sensitivity. *Geophys. Res. Lett.,* **31,** L03205, doi:10.1029/2003GL018747.

——, and M. Webb, 2008: Tropospheric adjustment induces a cloud component in CO_2 forcing. *J. Climate,* **21,** 58–71.

Hansen, J., M. Sato, and R. Ruedy, 1997: Radiative forcing and climate response. *J. Geophys. Res.,* **102** (D6), 6831–6864.

Huang, Y., 2013a: On the longwave climate feedbacks. *J. Climate,* **26,** 7603–7610.

——, 2013b: A simulated climatology of spectrally decomposed atmospheric infrared radiation. *J. Climate,* **26,** 1702–1715.

——, V. Ramaswamy, X. Huang, Q. Fu, and C. Bardeen, 2007a: A strict test in climate modeling with spectrally resolved radiances: GCM simulation versus AIRS observations. *Geophys. Res. Lett.,* **34,** L24707, doi:10.1029/2007GL031409.

——, ——, and B. Soden, 2007b: An investigation of the sensitivity of the clear-sky outgoing longwave radiation to atmospheric temperature and water vapor. *J. Geophys. Res.,* **112,** D05104, doi:10.1029/2005JD006906.

Ramaswamy, V., and Coauthors, 2001: Radiative forcing of climate change. *Climate Change 2001: The Scientific Basis,* J. T. Houghton et al., Eds., Cambridge University Press, 349–416.

Shell, K. M., J. T. Kiehl, and C. A. Shields, 2008: Using the radiative kernel technique to calculate climate feedbacks in NCAR's Community Atmospheric Model. *J. Climate,* **21,** 2269–2282.

Soden, B. J., I. M. Held, R. Colman, K. M. Shell, J. T. Kiehl, and C. A. Shields, 2008: Quantifying climate feedbacks using radiative kernels. *J. Climate,* **21,** 3504–3520.

Taylor, K. E., R. J. Stouffer, and G. A. Meehl, 2012: An overview of CMIP5 and the experiment design. *Bull. Amer. Meteor. Soc.,* **93,** 485–498.

Vial, J., J.-L. Dufresne, and S. Bony, 2013: On the interpretation of inter-model spread in CMIP5 climate sensitivity estimates. *Climate Dyn.,* **41,** 3339–3362, doi:10.1007/s00382-013-1725-9.

Webb, M. J., F. H. Lambert, and J. M. Gregory, 2013: Origins of differences in climate sensitivity, forcing and feedback in climate models. *Climate Dyn.,* **40,** 677–707, doi:10.1007/s00382-012-1336-x.

Wetherald, R. T., and S. Manabe, 1988: Cloud feedback processes in a general circulation model. *J. Atmos. Sci.,* **45,** 1397–1416.

WMO, 1957: Definition of the tropopause. *WMO Bull.,* **6,** 136.